Mitochondrial Dysfunction in Chronic Limb Ischemic Myopathy

Do Young Kim

Abstract

Critical limb ischemia (CLI), the most advanced clinical manifestation of peripheral arterial disease (PAD), is associated with cycles of ischemia and reperfusion (I/R) that are thought to compromise the bioenergetics of mitochondria. However, the specific biochemical mechanism through which the mitochondrial dysfunctions occur have not been fully characterized. In this experiment, the left femoral arteries of mice (n=3) were ligated and excised, and tibial anterior muscles were harvested on day 7 and 14. The sections were stained for hematoxylin and eosin (H&E), succinate dehydrogenase (SDH), and cytochrome C oxidase (COX). The results show significant increase in centralized nuclei in injured muscles compared to contralateral controls. SDH and COX data were inconclusive. Future studies are expected to continue identifying key mechanisms that link oxidative damage and mitochondrial dysfunction to develop targeted therapies that aim to improve the compromised bioenergetics of mitochondria, improving the prognosis of PAD and CLI patients.

Introduction

Peripheral Arterial Disease (PAD) is usually caused by atherosclerotic occlusive disease, where an artery develops a plaque that eventually blocks the circulation of blood[1]. While the disease is uncommon among population under the age of 50, it is estimated to affect more than 25% of the population over the age of 80[2]. The most severe cases of PAD, known as critical limb ischemia (CLI), are associated with 20% mortality rate at 1 year, and may require amputation among other surgeries[1,3,4]. There has been research performed to treat the symptoms through surgeries, physical therapies, and other walking regimens, but little is known about the exact mechanism and early progression of PAD[5].

In patients with PAD, the hypoxia induced by reduced blood flow results in ischemic muscle injuries, leading to muscle degeneration and the associated clinical symptoms[6,7]. An increasing number of researches have started to point to defective bioenergetics of mitochondria as an additional source of myopathy[8-11]. PAD patients undergo cycles of ischemia and reperfusion (I/R) where the blood flow is occluded during ischemia and reperfusion occurs when elevation of blood pressure pushes the blood through the blockage.

The lack and burst of oxygen in I/R cycles are associated with elevated levels of reactive oxygen species (ROS) that are thought to compromise the bioenergetics of the mitochondria, damaging it and further releasing ROS in "ROS-induced-ROS" positive feedback loop[8,12,13]. During ischemia, XO is the primary source of ROS, releasing $O_2^{\cdot -}$ during the conversion of hypoxanthine to xanthine[13]. The high oxygen supply at the beginning of reperfusion activates several sources (xanthine oxidase, p66Shc, mitochondrial K_{ATP} channels, and monoamine oxidases, among others) of ROS (mainly $O_2^{\cdot -}$, H_2O_2, $HO^{\cdot}$, NO, and peroxynitrite)[13-16]. Thus, the primary sources of ROS during I/R are complex I and III[13].

The resulting chronically elevated ROS is believed to be one of the causes of ischemic muscle injury[7,8,13]. The goal of this experiment is to elucidate a more direct relationship between CLI and mitochondrial damage through examination of mitochondrial complex II (succinate dehydrogenase) and IV (cytochrome C oxidase) in mice with surgically induced CLI. The results are expected to become the basis for future research aimed at identifying specific mitochondrial malfunctions that lead to ROS induced muscle degeneration in PAD patients, providing grounds for researching targeted therapeutics to slow or inhibit the myopathy in PAD.

Methods

To test and confirm that CLI induces mitochondrial dysfunction, adult mice underwent surgeries to ligate and excise the left femoral arteries between the hip and the ankle. On day 7 and 14 (n = 3), the mice were asphyxiated and the tibialis anterior (TA) muscles were harvested. The collected TA muscles were frozen in isomethylbutane cooled to viscous state by liquid nitrogen, freezing the muscle fibers in relaxed states. The frozen muscles were sectioned by cryostat (ThermoFisher CryoStar NX70) in 10 µm thickness, and serial sections were stained for Hematoxylin and Eosin (H&E), succinate dehydrogenase (SDH), and cytochrome C oxidase (COX).

For analysis, three random areas from each sample muscle section were photographed (20X). On each image, the number of fibers that had the desired quality was counted and divided over the total number of fibers in the image, leaving out fibers that are hard to quantify or and partially cut off by the image border. Using the right leg TA muscles as contralateral controls, the stained sections were compared for percentage of fibers with centralized nuclei (indication of muscle fiber regeneration) and the percentage of SDH^+ and COX^+ fibers. The quantified data was statistically tested using two-way analysis of variance (ANOVA; Tukey's multiple comparisons test).

Results

Centralized Nuclei

Originally, the centralized nuclei count data was only going to be compared within each sample (ex. Day 7 Mice 1's left muscle data with Day 7 Mice 1's right muscle data). However, two-way ANOVA showed no statistically significant differences ($p>0.95$) between the data from different mice of the same category. Based on this test, comparisons between the injured and the control muscles were done with pooled data.

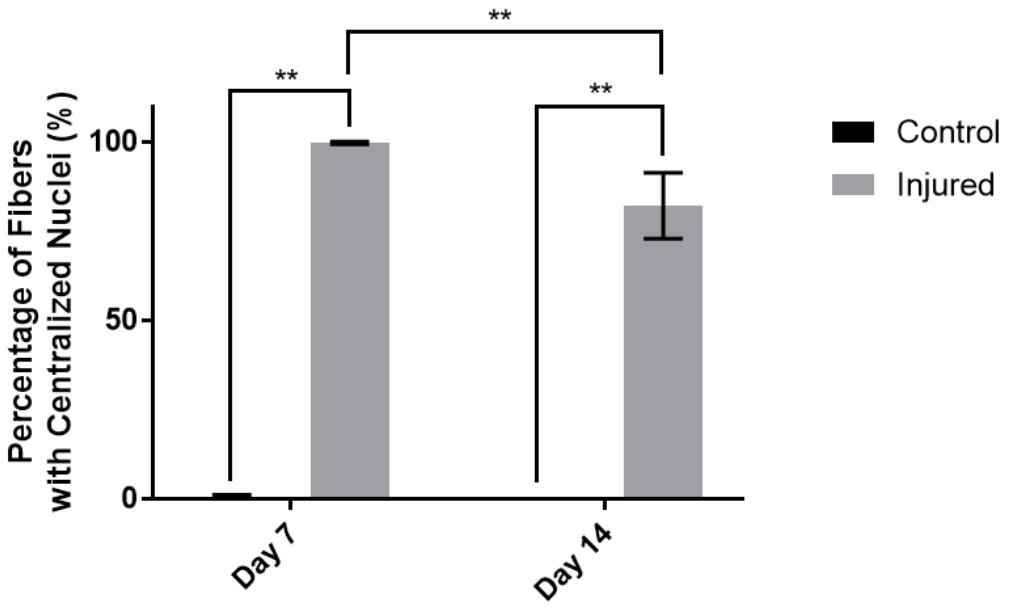

Figure 1. Percentage of fibers with centralized nuclei. Data are means ± SD, n=3 per day, **Tukey adjusted p<0.0001.

The percentage of centralized nuclei showed significant differences between the Control and the Injured samples on both Day 7 and 14 (Figure 1). The percentage of centralized nuclei also showed statistically significant decrease in the Injured samples between Day 7 and 14 (Figure 1).

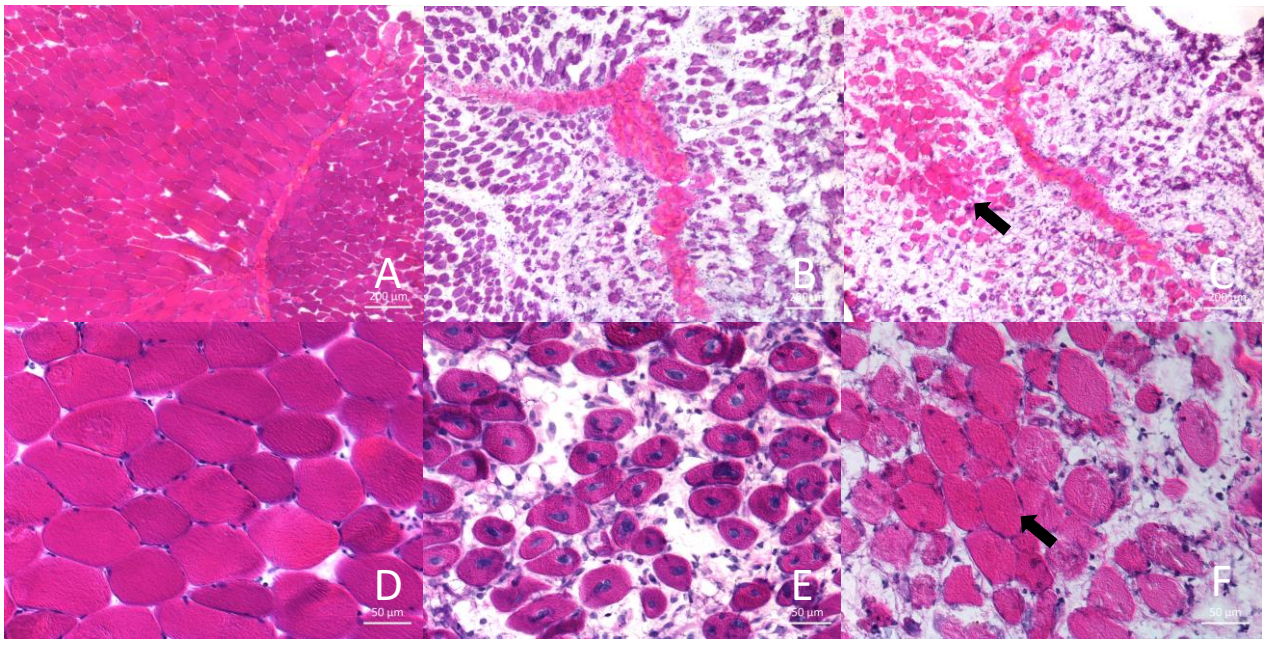

Figure 2. Day 7 H&E stain images showing normal myofibers in 5X (A) and 20X (D). CLI injured myofibers are shown in 5X (B) and (C), and 20X (E) and (F).

Day 7 H&E images showed considerable variation in the myofiber damage and regeneration between CLI injured mice samples (Figure 2). (B) and (E) are images from Mice #1 and (C) and (F) are from Mice #2. The images show much more new, purple muscle fibers with centralized nuclei in Mice #1 compared to Mice #2, which still show pink myofibers that are necrotizing (black arrow).

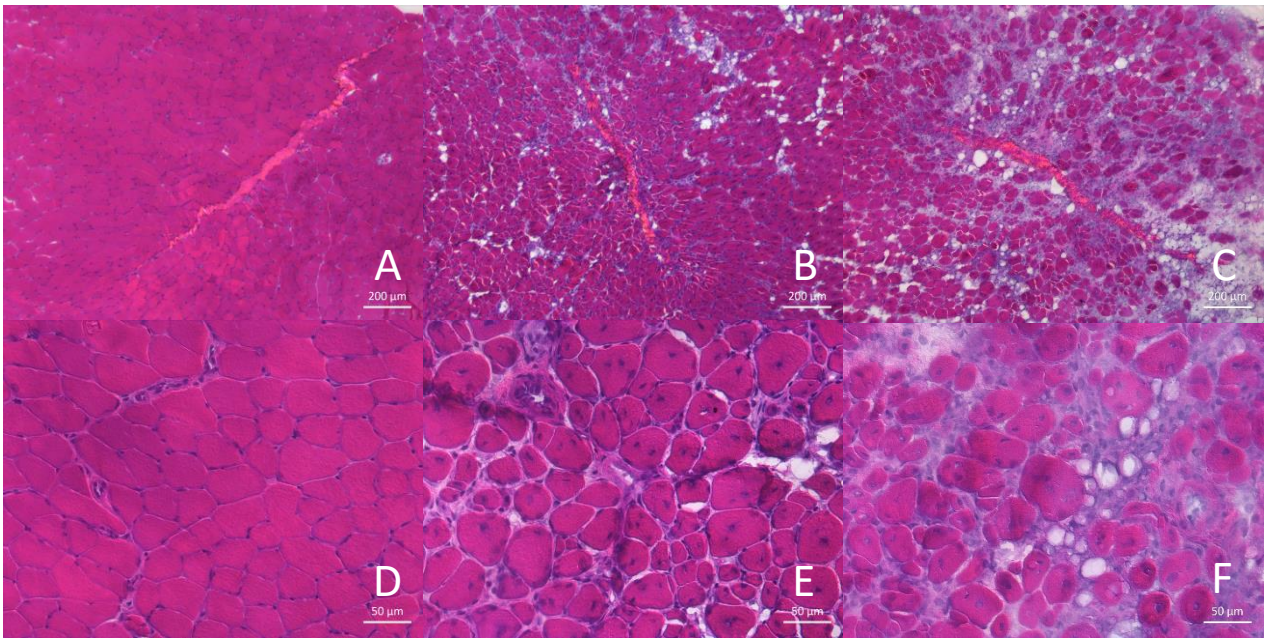

Figure 3. Day 14 H&E stain images showing normal myofibers in 5X (A) and 20X (D). CLI injured myofibers are shown in 5X (B) and (C), and 20X (E) and (F).

Day 14 images (Figure 3) showed less variation in myofiber damage and regeneration between CLI injured mice samples compared to Day 7 images (Figure 2). In Figure 3, (B) and (E) are from Mice # 4, and (C) and (F) are from Mice #5. Images from both Mice #4 and #5 still show a high concentration of centralized nuclei, but Mice #5 has extracellular matrix that is much more purple. This is most likely because not all of the myofiber fragmentation has been recovered, so some of the hematoxylin (purple staining for nuclei) leaked out.

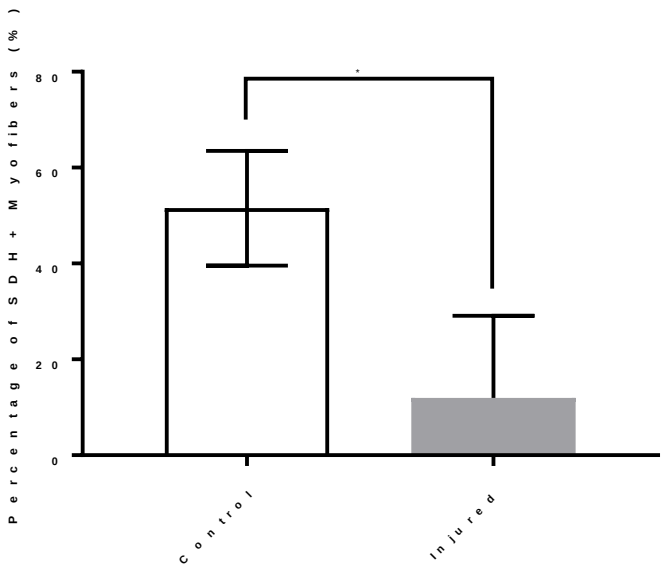

Figure 4. Percentage of SDH^+ fibers at Day 7. Data are means ± SD, n=3 per day, **Tukey adjusted $p<0.005$.

The percentage of SDH^+ fibers showed significant differences between the Control and the Injured samples on Day 7 (Figure 4). Day 14 data was not quantified due to technical difficulties (Figure 6).

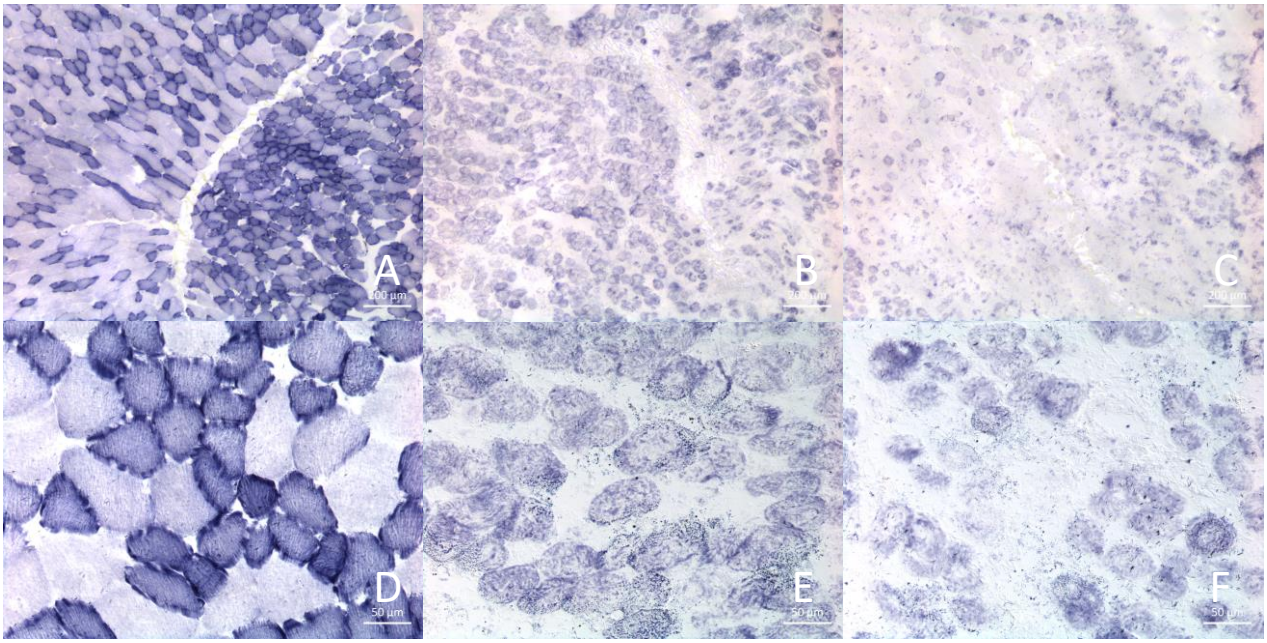

Figure 5. Day 7 SDH stain images showing normal myofibers in 5X (A) and 20X (D). CLI injured myofibers are shown in 5X (B) and (C), and 20X (E) and (F).

Day 7 SDH images (Figure 5) showed clear differences between control and CLI injured muscle sections. In Figure 5, (B) and (E) are images from Mice #1 and (C) and (F) are from Mice #2. Mice

#1 show slightly more SDH^+ fibers than Mice #2, which may correlate with the more advanced regeneration shown in Figure 2.

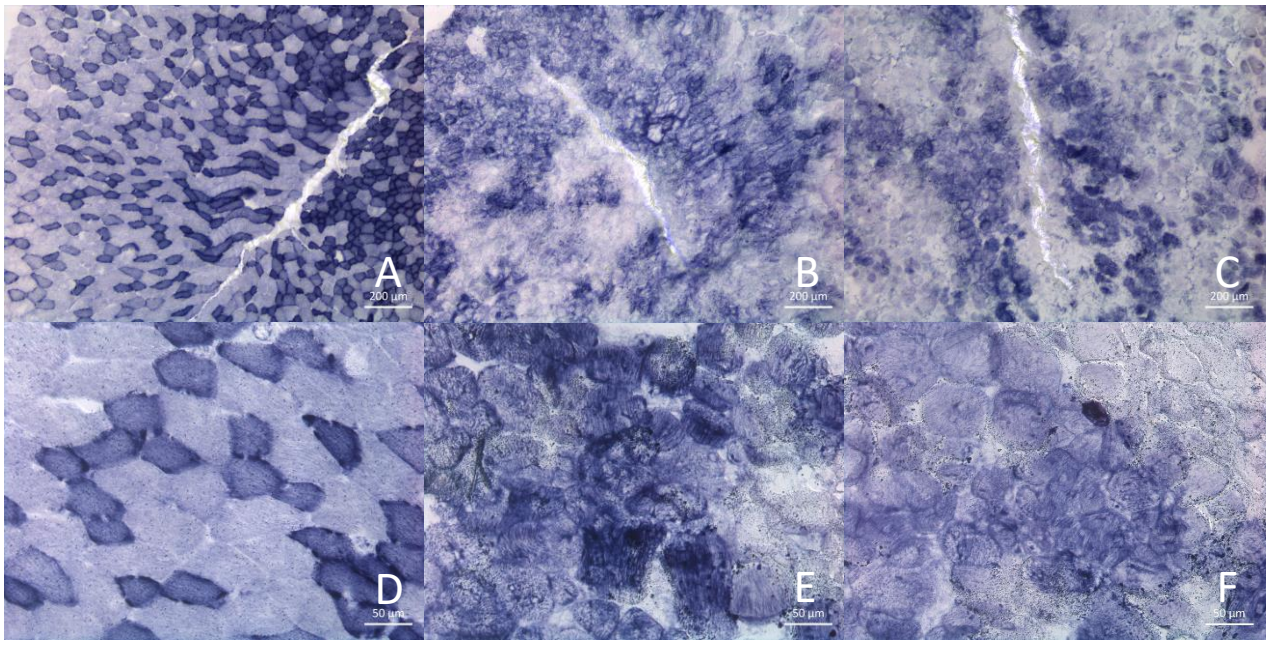

Figure 6. Day 14 SDH stain images showing normal myofibers in 5X (A) and 20X (D). CLI injured myofibers are shown in 5X (B) and (C), and 20X (E) and (F).

Day 14 SDH images (Figure 6) showed clear differences between control and CLI injured muscle sections. In Figure 6, (B) and (E) are images from Mice #4 and (C) and (F) are from Mice #5. The reason Day 14 SDH images were not quantified was because the outlines of muscle fibers (sarcolemma) were impossible to distinguish.

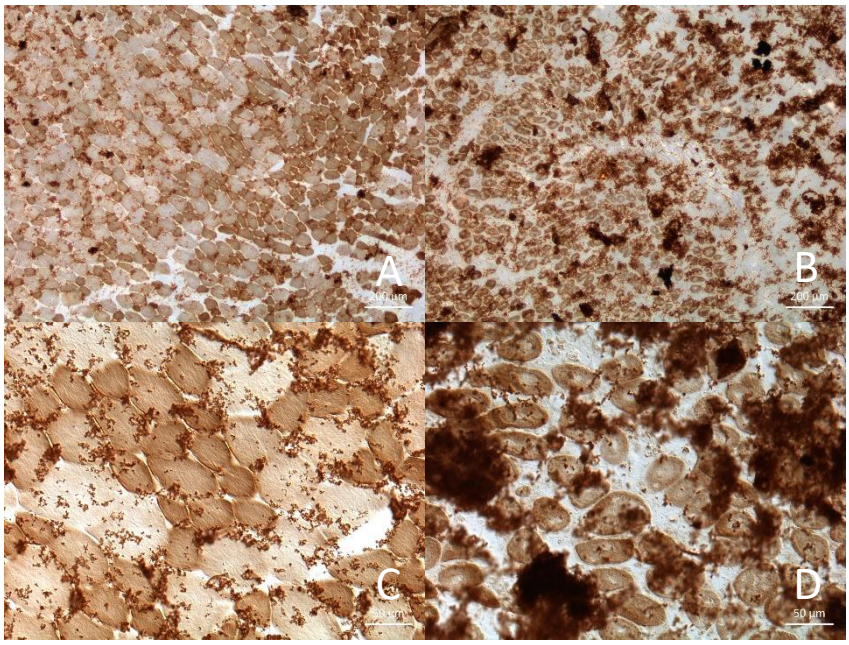

Figure 7. Day 7 COX stain images showing normal myofibers in 5X (A) and 20X (C). CLI injured myofibers are shown in 5X (B), and 20X (D).

Day 7 COX images (Figure 7) showed very clear residues, mostly likely from the COX media that was stored at -4°C for about two weeks. Pilot tests of COX staining had used freshly made COX media and did not have this residue issue, but unfortunately, the Jang Lab ran out of the supply of cytochrome C oxidase, the main enzyme component for COX staining media. Because the residues would make quantifications very unreliable, COX stainings were not quantified and Day 14 sections were not stained for COX.

Discussion

The goal of this experiment was to see how mitochondrial complex II (SDH) and IV (COX) are affected in mice with surgically induced critical limb ischemia. COX is a component of complex IV, which is encoded by both nuclear DNA (nDNA) and mitochondrial DNA (mtDNA); it reflects respiratory chain function. SDH (complex II) is encoded by nDNA and is a sign of mitochondrial proliferation. The most relevant study was performed by Pipinos et al. where he measured the activity of mitochondrial complexes I through IV between control and PAD patients' gastric muscle[8]. They found that all but complex II were significantly different[8], while is seemingly different than what the data in this experiment indicates. While the SDH and COX data were not fully obtained and quantified in this experiment, the Day 7 COX images hint at higher percentages of COX^+ fibers than SDH^+ fibers. If additional experiments do show the abundance of such COX^+ SDH^- fibers commonly know as ragged red fibers (RRF), it will indicate at least partly functional electron transport chain and compromise in mitochondria's ability to proliferate.

Three main things could be improved from this experiment. First, several studies have concluded that oxidative damage is myofiber type selective, where type II fast twitch and type I/II fibers are much more prone to oxidative damage than type I slow twitch fibers[17,18]. Tibial anterior muscle,

used in this experiment, is primarily glyosidic, with mostly type II fibers on the exterior and some type I fibers on the interior. Such regional distribution pattern makes taking random area photos for quantification much less effective in sampling for the whole section. To account for the additional independent variable (fiber type), it will be very helpful for future experiments to couple SDH and COX staining with myosin heavy chain (MHC) staining to see if the addition of the variable shows any new distinct patterns.

Second, to calculate fiber areas and to improve the quantifications of SDH and COX images, it will be very helpful to perform fluorescence staining of SDH and sarcolemma, as the SDH images from this experiment were difficult to accurately quantify because of the background noise and unidentifiable fiber outlines.

Third, a standard or an algorithm to distinguish between positive and negative fibers in SDH and COX staining are needed, as this experiment simply excluded the fibers that are shades of light blue. Originally, the light intensity of blue color (for SDH) and brown color (for COX) was going to be analyzed to distinguish between the positive and negative fibers in each staining. However, each section requires different amount of light intensity adjustment on the microscope to get the best image, so the base light intensity is not consistent across the different sections and samples. For this experiment, the images were quantified by hand, leaving much room for improvements in accuracy and precision.

In conclusion, although this study was not able to derive conclusive data, it offers multiple points that could be improved in follow up experiments. Such future experiments will contribute to an understanding of the underlying biochemical mechanism through which mitochondrial bioenergetics is compromised by oxidative damage, providing grounds for developing targeted mitochondrial therapies for PAD and CLI patients[19].

References

1 Schirmang, T. C., Ahn, S. H., Murphy, T. P., Dubel, G. J. & Soares, G. M. Peripheral arterial disease: update of overview and treatment. *Medicine and health, Rhode Island* **92**, 398-402 (2009).

2 Allison, M. A. *et al.* Ethnic-specific prevalence of peripheral arterial disease in the United States. *American journal of preventive medicine* **32**, 328-333, doi:10.1016/j.amepre.2006.12.010 (2007).

3 Teraa, M., Conte, M. S., Moll, F. L. & Verhaar, M. C. Critical Limb Ischemia: Current Trends and Future Directions. *Journal of the American Heart Association* **5**, doi:10.1161/jaha.115.002938 (2016).

4 Dormandy, J., Heeck, L. & Vig, S. The fate of patients with critical leg ischemia. *Seminars in vascular surgery* **12**, 142-147 (1999).

5 Criqui, M. H. & Aboyans, V. Epidemiology of peripheral artery disease. *Circulation research* **116**, 1509-1526, doi:10.1161/circresaha.116.303849 (2015).

6 Regensteiner, J. G. *et al.* Chronic changes in skeletal muscle histology and function in peripheral arterial disease. *Circulation* **87**, 413-421, doi:10.1161/01.cir.87.2.413 (1993).

7 Ryan, T. E. *et al.* Mitochondrial Regulation of the Muscle Microenvironment in Critical Limb Ischemia. *Frontiers in physiology* **6**, 336, doi:10.3389/fphys.2015.00336 (2015).

8 Pipinos, II *et al.* Mitochondrial defects and oxidative damage in patients with peripheral arterial disease. *Free radical biology & medicine* **41**, 262-269, doi:10.1016/j.freeradbiomed.2006.04.003 (2006).

9 Kemp, G. *Mitochondrial dysfunction in chronic ischemia and peripheral vascular disease*. Vol. 4 (2004).

10 Kwong, L. K. & Sohal, R. S. Substrate and Site Specificity of Hydrogen Peroxide Generation in Mouse Mitochondria. *Archives of Biochemistry and Biophysics* **350**, 118-126, doi:https://doi.org/10.1006/abbi.1997.0489 (1998).

11 Lenaz, G., Bovina, C., Formiggini, G. & Parenti Castelli, G. Mitochondria, oxidative stress, and antioxidant defences. *Acta biochimica Polonica* **46**, 1-21 (1999).

12 Kalogeris, T., Bao, Y. & Korthuis, R. J. Mitochondrial reactive oxygen species: a double edged sword in ischemia/reperfusion vs preconditioning. *Redox biology* **2**, 702-714, doi:10.1016/j.redox.2014.05.006 (2014).

13 Paradis, S. *et al.* Chronology of mitochondrial and cellular events during skeletal muscle ischemia-reperfusion. *American journal of physiology. Cell physiology* **310**, C968-982, doi:10.1152/ajpcell.00356.2015 (2016).

14 de Groot, H. & Rauen, U. Ischemia-reperfusion injury: processes in pathogenetic networks: a review. *Transplantation proceedings* **39**, 481-484, doi:10.1016/j.transproceed.2006.12.012 (2007).

15 Gute, D. C., Ishida, T., Yarimizu, K. & Korthuis, R. J. Inflammatory responses to ischemia and reperfusion in skeletal muscle. *Molecular and cellular biochemistry* **179**, 169-187 (1998).

16 Kalogeris, T., Baines, C. P., Krenz, M. & Korthuis, R. J. Cell biology of ischemia/reperfusion injury. *International review of cell and molecular biology* **298**, 229-317, doi:10.1016/b978-0-12-394309-5.00006-7 (2012).

17 Casale, G. P. *et al.* Fiber Type-Selective Oxidative Damage and Myofiber Atrophy in the Gastrocnemius of Patients with Peripheral Arterial Disease. *The FASEB Journal* **25**, 1092.1024-1092.1024, doi:10.1096/fasebj.25.1_supplement.1092.24 (2011).

18 Koutakis, P. *et al.* Oxidative damage in the gastrocnemius of patients with peripheral artery disease is myofiber type selective. *Redox biology* **2**, 921-928, doi:https://doi.org/10.1016/j.redox.2014.07.002 (2014).

19 Chouchani, E. T. *et al.* Ischaemic accumulation of succinate controls reperfusion injury through mitochondrial ROS. *Nature* **515**, 431-435, doi:10.1038/nature13909 (2014).